$T_{4,4,4}$-graphyne : a 2D carbon allotrope with an intrinsic direct bandgap

Accepted Manuscript

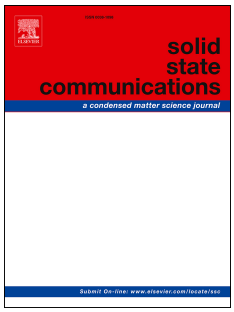

$T_{4,4,4}$-graphyne: A 2D carbon allotrope with an intrinsic direct bandgap

Weiyang Wang, Linyang Li, Xiangru Kong, B. Van Duppen, F.M. Peeters

PII: S0038-1098(18)30636-7

DOI: https://doi.org/10.1016/j.ssc.2019.02.001

Reference: SSC 13590

To appear in: *Solid State Communications*

Received Date: 31 August 2018

Accepted Date: 5 February 2019

Please cite this article as: W. Wang, L. Li, X. Kong, B. Van Duppen, F.M. Peeters, $T_{4,4,4}$-graphyne: A 2D carbon allotrope with an intrinsic direct bandgap, *Solid State Communications* (2019), doi: https://doi.org/10.1016/j.ssc.2019.02.001.

$T_{4,4,4}$-graphyne: A 2D carbon allotrope with an intrinsic direct bandgap

Weiyang Wang[a,b], Linyang Li[b,*], Xiangru Kong[c], B. Van Duppen[b], and F M. Peeters[d,b]

[a] School of Physics and Electronics Information, Shangrao Normal University, Shangrao, Jiangxi 334001,China

[b] Departement Fysica, Universiteit Antwerpen, Groenenborgerlaan 171, B-2020 Antwerpen, Belgium

[c] International Center of Quantum Materials, Peking University, 100871 Beijing, China

[d] School of Physics and Astronomy and Yunnan Key Laboratory for Quantum Information, Yunnan University, Kunming 650091, China

Wang.Weiyang.CMT@foxmail.com (Weiyang Wang)
linyang.li@uantwerpen.be (Linyang Li)
kongxru@pku.edu.cn (Xiangru Kong)
ben.vanduppen@uantwerpen.be (B. Van Duppen)
francois.peeters@uantwerpen.be (F M. Peeters)

$T_{4,4,4}$-graphyne: A 2D carbon allotrope with an intrinsic direct bandgap

Weiyang Wang[a,b], Linyang Li[b,*], Xiangru Kong[c], B. Van Duppen[b], F M. Peeters[d,b]

[a]*School of Physics and Electronics Information, Shangrao Normal University, Shangrao, Jiangxi 334001, China*
[b]*Departement Fysica, Universiteit Antwerpen, Groenenborgerlaan 171, B-2020 Antwerpen, Belgium*
[c]*International Center of Quantum Materials, Peking University, 100871 Beijing, China*
[d]*School of Physics and Astronomy and Yunnan Key Laboratory for Quantum Information, Yunnan University, Kunming 650091, China*

Abstract

A novel two-dimensional (2D) structurally stable carbon allotrope is proposed using first-principles calculations, which is a promising material for water purification and for electronic devices due to its unique porous structure and electronic properties. Rectangular and hexagonal rings are connected with acetylenic linkages, forming a nanoporous structure with a pore size of 6.41 Å, which is known as $T_{4,4,4}$-graphyne. This 2D sheet exhibits a direct bandgap of 0.63 eV at the M point, which originates from the p_z atomic orbitals of carbon atoms as confirmed by a tight-binding model. Importantly, $T_{4,4,4}$-graphyne is found to be energetically more preferable than the experimentally realized β-graphdiyne, it is dynamically stable and can withstand temperatures up to 1500 K.

Keywords: Graphyne, Semiconductor, Nanoporous structure, First-principles calculation.

1. Introduction

Carbon atoms have been known to form a variety of structural allotropes of different dimensionalities due to the ability of forming a large variety

*linyang.li@uantwerpen.be

of different hybridizations, resulting in zero-dimensional fullerene [1], one-dimensional carbon nanotube [2], two-dimensional (2D) graphene [3], and three-dimensional diamond. Among these allotropes, graphene has attracted tremendous attention predominantly due to its superior electronic and optical properties [4]. Its peculiar band structure features so-called Dirac cones that are a direct consequence of its hexagonal crystal symmetry [5], making it a promising material for carbon-based devices [6, 7, 8]. However, graphene is a semimetal with zero bandgap which greatly limits its application in logic devices [9]. It is impossible to turn off a transistor if the basic material has no bandgap. Therefore extensive work has been devoted to open up a bandgap in graphene-like materials. These include hydrogenating graphene to graphane [10], cutting graphene into nanoribbon [11], fabricating graphene quantum dot [12], doping graphene with extra atoms [13, 14], and applying external stress on graphene [15]. These approaches can create a narrow bandgap and some of them may destroy the hexagonal honeycomb structure of graphene and often degrades its electronic performance. Therefore, it is desirable to search for novel 2D carbon allotropes with a direct bandgap.

Recently, graphyne structures, composed of both sp and sp^2 hybridized carbon atoms, have been investigated. Graphyne possesses various structures [16, 17, 18, 19, 20, 21, 22, 23, 24, 25] arising from the ratio and arrangement of sp and sp^2 carbon atoms [26], which leads to very different band structures. According to its band structure, graphyne can be classified into three classes: (i) metal, such as R-graphyne [17]; (ii) semimetal having Dirac points which is similar to graphene, such as α- β-, and δ-graphynes [18, 19, 20, 21]; and (iii) semiconductor with a bandgap, such as γ-graphyne and γ-graphdiyne [27, 28]. Both γ-graphyne and γ-graphdiyne possess a direct bandgap of, respectively, 0.46 eV [27, 28, 29, 30, 31, 32] and 0.48 eV [27, 28, 33, 34] as calculated at the Perdew-Burke-Ernzerhof (PBE) level, while with Heyd-Scuseria-Ernzerhof (HSE06) hybrid functionals these values are, respectively, increased to 0.96 eV [27, 28, 31, 32] and 0.89 eV [28, 35], which is comparable to that of Si. One advantage of γ-graphyne and γ-graphdiyne over Si is that they have a direct bandgap, which results in a higher light absorption efficiency and a higher radiative recombination rate. From this perspective, both γ-graphyne and γ-graphdiyne are more suitable for applications in electronic devices than graphene [36, 37]. Moreover, γ-graphyne-n, unlike graphene, naturally possess uniform and controllable pore-size distribution with high membrane porosity as well as mechano-chemical stability. This unique structure enables γ-graphyne-n to be used as a promising material in applications [27, 28], such

as catalysis [38, 39], lithium storage [40, 41], and gas separation [42, 43, 44] as well as water purification [45, 46, 47, 48, 49]. γ-graphyne as well as γ- and β-graphdiynes have been already fabricated[50, 51, 52]. The successful synthesis of new graphyne structures have inspired further search for other 2D carbon allotropes through both experimental techniques and theoretical calculations, especially for exploring new graphyne structures with a direct bandgap and with intrinsic subnanometer pores.

In this paper, we employ first-principles calculations to design new structurally stable 2D carbon networks composed of sp and sp^2 hybridized atoms. According to its structure, we call it $T_{4,4,4}$-graphyne. This 2D material is energetically more favorable than the experimentally realized β-graphdiyne and is found to be dynamical as well as thermal stable. Different from graphene, $T_{4,4,4}$-graphyne has a direct bandgap of 0.63 eV at the M point. This bandgap arises from p_z atomic orbitals of carbon atoms confirmed by both orbital-projected band structure and tight-binding (TB) model. The porous structure exhibits a periodic array of holes of diameter 6.41 Å.

2. Computational details

The first-principles calculations within the framework of density functional theory (DFT) are carried out using the Vienna *ab initio* simulation package (VASP) [53]. The electron exchange-correlation functional is treated by using the generalized gradient approximation (GGA) within the PBE parameterization [54]. An energy cutoff of 520 eV for the plane wave basis with an energy precision of 10^{-5} eV is adopted for all the calculations. The first Brillouin zone (BZ) is sampled with a $15 \times 15 \times 1$ Γ-centered Monkhorst-Pack grid. During geometry optimization, both atomic positions and lattice vectors are fully optimized using the conjugate gradient scheme until the maximum force on each atom is less than 0.01 eV/Å. To avoid image interactions from the periodic boundary condition, a large vacuum space of at least 17 Å is applied to the perpendicular direction of the 2D layer. Phonon calculations by the supercell approach as implemented in the PHONOPY code [55] are used to evaluate the dynamical stability.

3. Numerical results and discussions

3.1. Structure and stability

The optimized crystal structure of the 2D carbon allotrope monolayer is shown in Fig. 1(a). The top view shows that the monolayer is composed of

hexagonal carbon rings surrounded by three rectangular carbon rings [56] and triple bonds of carbon. According to the name rules [26], it should be called $4,4,4$-graphyne. As it belongs to the 2D trigonal lattice, we call it $T_{4,4,4}$-graphyne. Besides the carbon atoms (sp) in the triple bonds, the other carbon atoms are sp^2. It is noted that $T_{4,4,4}$-graphyne exhibits slightly distorted bond lengths and bond angles when compared with the regular bond parameters formed by sp and sp^2 hybridization in graphene and graphynes [26]. For example, the bond angle between the neighboring single bond and triple bond is 170.3° and the four angles in rectangular rings are not 90°. The triple bond length ($d_1 = 1.253$ Å) is close to the sp hybridized bond length of the previous investigated graphyne structures ($1.21 \sim 1.24$ Å) [57], shorter than the rest of bond lengths, namely, $d_2 = 1.343$ Å, $d_3 = 1.507$ Å, $d_4 = 1.459$ Å, $d_5 = 1.466$ Å, and $d_6 = 1.378$ Å, due to the stabilization effect of the triple bonds. Moreover, $d_2 - d_6$ do not deviate significantly from the sp^2 hybridized bond length of graphene (1.42 Å), due to retaining the close sp^2 hybridization of these carbon atoms.

The $T_{4,4,4}$-graphyne monolayer can be described by the plane group p-$6m2$ (space group no. 187) with an optimized lattice constant of $a = b = 9.292$ Å and its unit cell contains 18 carbon atoms as shown by the blue dashed quadrangle in Fig. 1(a). Importantly, it shows a nanoporous structure and the pore diameter of the circumcircle is about $l = 6.41$ Å, close to that of bare γ-graphyne-3 (6.9 Å) which has been proposed for seawater desalination [45, 46]. The filter application results from the diameter of hydration structures of ions which is larger than the pore size of the single-layer γ-graphyne-3 membranes, so that ion passage is blocked, whereas water unimpeded flows through the membrane due to its smaller size. Moreover, it is demonstrated that the salt rejection decreases with increasing n for pristine γ-graphyne-n when $n \geq 3$ [46], suggesting that the pore size of $T_{4,4,4}$-grahpyne sheet is most suitable for water purification. Recently, it is also found that hydrogenated α-graphyne and γ-graphyne-n with $2 \leq n \leq 4$ membranes exhibit an improved salt rejection performance as compared to the pristine one due to their lower pore area [47]. Thus, monolayer $T_{4,4,4}$-graphyne is expected to have great potential as a membrane for water purification.

Due to the presence of sp-hybridized carbon atoms, graphyne monolayers are energetically less favorable than graphene. Here, we compare the total energy E_t of $T_{4,4,4}$-graphyne with that of some 2D carbon allotropes to evaluate the energetic stability of $T_{4,4,4}$-graphyne. So far, γ-graphyne as well as γ- and β-graphdiynes have been realized experimentally [50, 51, 52],

which possess respectively $E_t = -8.58$, -8.49, and -8.31 eV/atom. In contrast, the E_t of $T_{4,4,4}$-graphyne is -8.44 eV/atom, which is comparable to that of γ-graphdiyne and much lower than that of β-graphdiyne. The energetic favorability of $T_{4,4,4}$-graphyne over β-graphdiyne is ascribed to the presence of hexagonal carbon rings. This is promising for future realization of $T_{4,4,4}$-graphyne.

To confirm the dynamic stability, we calculated the phonon spectrum of monolayer $T_{4,4,4}$-graphyne. Fig. 1(b) clearly shows that the phonon spectrum is free from imaginary phonon modes along the highly symmetric direction in the first BZ, confirming the dynamical stability of $T_{4,4,4}$-graphyne. To further check the thermal stability, first-principles MD simulations are performed using the Nosé-Hoover method [53] at different temperatures with the time scale of 1 fs, as shown in Fig. 2. It shows that the E_t of $T_{4,4,4}$-graphyne monolayer with $3 \times 3 \times 1$ supercell is stable throughout the simulation. Snapshots of the geometries at the end of 5 ps simulations show that the carbon atoms of $T_{4,4,4}$-graphyne are slightly displaced from their equilibrium positions at temperature up to 1500 K. However, the well-preserved geometry of $T_{4,4,4}$-graphyne monolayer at such high temperature suggests that $T_{4,4,4}$-graphyne is thermal stable and therefore has great potential for applications at high temperature.

3.2. Band structure

The electronic band structures of monolayer $T_{4,4,4}$-graphyne along the high symmetry lines in the first BZ is shown in Fig. 3. The solid curves formed by spheres represent the orbital-projected band structure calculated at the PBE level, where blue and pink solid curves arise from the contributions of p_z and $s + p_x + p_y$ atomic orbitals of carbon atoms, respectively. It is clear that $T_{4,4,4}$-graphyne has a direct bandgap of 0.34 eV (PBE) at the M point, indicating that $T_{4,4,4}$-graphyne is a direct gap semiconductor, similar to γ-graphyne which has a direct bandgap of 0.46 eV (PBE) at the same point [29, 30, 31, 32]. The energy bands close to the Fermi level originate from p_z atomic orbitals of the carbon atoms, and the couplings between p_z orbitals lead to the formation of a π-conjugated framework. For 2D carbon allotropes with Dirac band structures, the energy bands close to the Fermi level come from the contributions of p_z atomic orbitals, such as in the case of α-, β-, and $H_{4,4,4}$-graphynes. Besides monolayer γ-graphyne-n, graphyne structures with a direct bandgap are rare.

We adopt a simple TB Hamiltonian of π-electron of $T_{4,4,4}$-graphyne following Ref. [58]

$$H = \sum_i \varepsilon_i c_i^+ c_i - \sum_{<i,j>} t_{ij} \left(c_i^+ c_i + h.c. \right), \tag{1}$$

where ε_i, c_i^+, and c_i are, respectively, the on-site energy, creation operator, and annihilation operator of an electron at ith atom, and t_{ij} is the hopping energy of an electron between the ith and jth atoms. For simplicity, we omit the on-site energy difference of an electron in different hybridized carbon atoms and set it as zero in the calculation. According to the nearest-neighbor approximation, the distance-dependent hopping parameters can be classified into six types and determined by the formula $t_i = t_0 e^{q \cdot (1 - d_i/d_0)}$ [59] with $i = 1, 2, \cdots, 6$, where $t_0 = 2.7$ eV, $q = 2.2$, and $d_0 = 1.5$ Å. In this way, the electronic band structure of $T_{4,4,4}$-graphyne can be obtained by diagonalizing the Hamiltonian which becomes a 18×18 dimensional matrix in reciprocal space. The results are presented in Fig. 3 by the green dashed curves. The electronic band structure calculated by the TB model is in good agreement with that of our DFT calculation in the vicinity of the Fermi level, especially the direct bandgap at the M point. For γ-graphyne and γ-graphdiyne, the TB model shows that its bandgap originates from the difference of the hopping parameters and a Dirac point appears when all hopping parameters have the same value [58, 60]. However, our TB results show that the Dirac point is still absent when an homogeneous hopping parameter is adopted (see Fig. S1 in supplementary information). This indicates that the bandgap of $T_{4,4,4}$-graphyne comes from its peculiar periodic structure.

It is well known that the DFT-PBE calculations usually underestimate the bandgap of semiconductors when compared with experiment. For this reason, we use the more sophisticated HSE06 [61, 62] hybrid functionals, which gives more accurate prediction of semiconductor bandgap. The calculation result is shown in Fig. 4, which is similar to that of PBE calculation, except for a larger bandgap of 0.63 eV. This confirms that $T_{4,4,4}$-graphyne has potential applications in semiconductor electronic devices.

4. Conclusions

By using first-principles calculations in combination with a TB model, we predict a new carbon monolayer called $T_{4,4,4}$-graphyne which is a direct

semiconductor with: 1) a nanoporous structure with pore size of 6.41 Å, 2) has a high stability, and 3) a direct bandgap of 0.63 eV. The nanoporous structure has potential applications for water purification. The structural stability is confirmed by our comprehensive study of the energetic, dynamic, and thermal properties of $T_{4,4,4}$-graphyne. The direct bandgap, originating from p_z atomic orbitals of carbon atoms, makes $T_{4,4,4}$-graphyne a promising material for semiconductor electronic devices. A simple TB model was constructed and it shows that the origin of the bandgap is the peculiar periodic structure of $T_{4,4,4}$-graphyne, which is different from that of γ-graphyne and γ-graphdiyne.

Acknowledgments

This work was supported by National Natural Science Foundation of China (Grant Nos. 11404214 and 11455015), the China Scholarship Council (CSC), the Fonds voor Wetenschappelijk Onderzoek (FWO-V1), and the FLAG-ERA project TRANS2DTMD. BVD was supported by the Research Foundation - Flanders (FWO-Vl) through a postdoctoral fellowship. The computational resources and services used in this work were provided by the VSC (Flemish Supercomputer Center), funded by the Research Foundation - Flanders (FWO) and the Flemish Government - department EWI.

[1] H. W. Kroto, J. R. Heath, S. C. O'Brien, R. F. Curl, R. E. Smalley, C_{60}: Buckminsterfullerene, Nature 318 (1985) 162-163.

[2] S. Iijima, Helical microtubules of graphitic carbon, Nature 354 (1991) 56-58.

[3] K. S. Novoselov, A. K. Geim, S. V. Morozov, D. Jiang, Y. Zhang, S. V. Dubonos, I. V. Grigorieva, A. A. Firsov, Electric field effect in atomically thin carbon films, Science 306 (2004) 666-669.

[4] A. H. Castro Neto, F. Guinea, N. M. R. Peres, K. S. Novoselov, A. K. Geim, The electronic properties of graphene, Rev. Mod. Phys. 81 (2009) 109.

[5] A. K. Geim, Graphene: status and prospects, Science 324 (2009) 1530-1534.

[6] P. Avouris, Graphene: Electronic and photonic properties and devices, Nano Lett. 10 (2010) 4285-4294.

[7] G. Fiori, F. Bonaccorso, G. Iannaccone, T. Palacios, D. Neumaier, A. Seabaugh, S. K. Banerjee, L. Colombo, Electronics based on two-dimensional materials, Nat. Nanotechnol. 9 (2014) 768-779.

[8] U. Khan, T. Kim, H. Ryu, W. Seung, S. Kim, Graphene tribotronics for electronic skin and touch screen applications, Adv. Mater. 29 (2017) 1603544.

[9] D. J. Appelhans, Z. Lin, M. T. Lusk, Two-dimensional carbon semiconductor: Density functional theory calculations, Phys. Rev. B 82 (2010) 073410.

[10] D. C. Elias, R. R. Nair, T. M. G. Mohiuddin, S. V. Morozov, P. Blake, M. P. Halsall, A. C. Ferrari, D. W. Boukhvalov, M. I. Katsnelson, A. K. Geim, K. S. Novoselov, Control of graphene's properties by reversible hydrogenation: evidence for graphane, Science 323 (2009) 610-613.

[11] L. Tapasztó, G. Dobrik, P. Lambin, L. P. Biró, Tailoring the atomic structure of graphene nanoribbons by scanning tunnelling microscope lithography, Nat. Nanotechnol. 3 (2008) 397-401.

[12] L. A. Ponomarenko, F. Schedin, M. I. Katsnelson, R. Yang, E. W. Hill, K. S. Novoselov, A. K. Geim, Chaotic Dirac billiard in graphene quantum dots, Science 320 (2008) 356-358.

[13] S. Agnoli, M. Favaro, Doping graphene with boron: A review of synthesis methods, physicochemical characterization, and emerging applications, J. Mater. Chem. A 4 (2016) 5002-5025.

[14] J. H. Kim, D. H. Shin, H. S. Lee, C. W. Jang, J. M. Kim, S. W. Seo, S. Kim, S. Choi, Enhancement of efficiency in graphene/porous silicon solar cells by co-doping graphene with gold nanoparticles and bis(trifluoromethanesulfonyl)-amide, J. Mater. Chem. C 5 (2017) 9005-9011.

[15] C. Si, Z. Sun, F. Liu, Strain engineering of graphene: a review, Nanoscale 8 (2016) 3207-3217.

[16] A. Wang, L. Li, X. Wang, H. Bu, M. Zhao, Graphyne-based carbon allotropes with tunable properties: From Dirac fermion to semiconductor, Diam. Rel. Mat. 41 (2014) 65-72.

[17] W. Yin, Y. Xie, L. Liu, R. Wang, X. Wei, L. Lau, J. Zhong, Y. Chen, R-graphyne: a new two-dimensional carbon allotrope with versatile Dirac-like point in nanoribbons, J. Mater. Chem. A 1 (2013) 5341-5346.

[18] D. Malko, C. Neiss, F. Viñes, A. Görling, Competition for graphene: Graphynes with direction-dependent Dirac cones, Phys. Rev. Lett. 108 (2012) 086804.

[19] O. Leenaerts, B. Partoens, F. M. Peeters, Tunable double Dirac cone spectrum in bilayer α-graphyne, Appl. Phys. Lett. 103 (2013) 013105.

[20] H. Huang, W. Duan, Z. Liu, The existence/absence of Dirac cones in graphynes, New J. Phys. 15 (2013) 023004.

[21] M. Zhao, W. Dong, A. Wang, Two-dimensional carbon topological insulators superior to graphene, Sci. Rep. 3 (2013) 3532.

[22] L. Z. Zhang, Z. F. Wang, Z. M. Wang, S. X. Du, H. -J. Gao, F. Liu, Highly anisotropic Dirac fermions in square graphynes, J. Phys. Chem. Lett. 6 (2015) 2959-2962.

[23] N. V. R. Nulakani, V. Subramanian, Cp-graphyne: a low-energy graphyne polymorph with double distorted Dirac points, ACS Omega 2 (2017) 6822-6830.

[24] L. Li, X. Kong, F. M. Peeters, New nanoporous graphyne monolayer as nodal line semimetal: double Dirac points with an ultrahigh fermi velocity, (2018), arXiv:1803.06595.

[25] X. Niu, X. Mao, D. Yang, Z. Zhang, M. Si, D. Xue, Dirac cone in α-graphdiyne: a first-principles study, Nanoscale Res. Lett. 8 (2013) 469.

[26] R. H. Baughman, H. Eckhardt, M. Kertesz, Structure-property predictions for new planar forms of carbon: Layered phases containing sp^2 and sp atoms, J. Chem. Phys. 87 (1987) 6687.

[27] C. Huang, Y. Li, N. Wang, Y. Xue, Z. Zuo, H. Liu, Y. Li, Progress in research into 2D graphdiyne-based materials, Chem. Rev. 118 (2018) 7744-7803.

[28] J. Kang, Z. Wei, J. Li, Graphyne and its family: Recent theoretical advances, ACS Appl. Mater. Interfaces (2018) 8b03338, DOI: 10.1021/acsami.8b03338.

[29] J. M. Ducéré, C. Lepetit, R. Chauvin, Carbo-graphite: Structural, mechanical, and electronic properties, J. Phys. Chem. C 117 (2013) 21671-21681.

[30] A. R. Puigdollers, G. Alonso, P. Gamallo, First-principles study of structural, elastic and electronic properties of α-, β- and γ-graphyne, Carbon 96 (2016) 879-887.

[31] J. Kang, J. Li, F. Wu, S. S. Li, J. B. Xia, Elastic, electronic, and optical properties of two-dimensional graphyne sheet, J. Phys. Chem. C 115 (2011) 20466-20470.

[32] X. Deng, J. Zeng, M. Si, W. Lu, Band gap modulation in γ-graphyne by p-n codoping, EPL 115 (2016) 27009.

[33] P. Yang, Mechanical properties of graphdiyne sheet, Physica B 407 (2012) 4436-4439.

[34] L. Sun, P. H. Jiang, H. J. Liu, D. D. Fan, J. H. Liang, J. Wei, L. Cheng, J. Zhang, J. Shi, Graphdiyne: A two-dimensional thermoelectric material with high figure of merit, Carbon 90 (2015) 255-259.

[35] Q. Yue, S. Chang, J. Kang, S. Qin, J. Li, Mechanical and electronic properties of graphyne and its family under elastic strain: theoretical predictions, J. Phys. Chem. C 117 (2013) 14804-14811.

[36] D. Wu, Q. Liu, H. Fu, R. Wu, How to realize a spin-dependent Seebeck diode effect in metallic zigzag γ-graphyne nanoribbons?, Nanoscale 9 (2017) 18334-18342.

[37] J. Li, L. Xu, Y. Yang, X. Liu, Z. Yang, The transport and optoelectronic properties of γ-graphyne-based molecular magnetic tunnel junctions, Carbon 132 (2018) 632-640.

[38] X. Kong, Y. Huang, Q. Liu, Two-dimensional boron-doped graphyne nanosheet: A new metal-free catalyst for oxygen evolution reaction, Carbon 123 (2017) 558-564.

[39] X. Chen, Z. Lin, Single-layer graphdiyne-covered Pt(111) surface: improved catalysis confined under two-dimensional overlayer, J. Nanopart. Res 20 (2018) 136.

[40] S. Kumar, T. J. D. Kumar, Electronic structure calculations of hydrogen storage in lithiumdecorated metal-graphyne framework, ACS Appl. Mater. Interfaces 9 (2017) 28659-28666.

[41] J. He, N. Wang, Z. Cui, H. Du, L. Fu, C. Huang, Z, Yang, X. Shen, Y. Yi, Z. Tu, Y. Li, Hydrogen substituted graphdiyne as carbon-rich flexible electrode for lithium and sodium ion batteries, Nat. Commun. 8 (2017) 1172.

[42] W. Zhao, L. Yuan, J. Yang, Graphdiyne as hydrogen purification membrane, Chin. J. Chem. Phys. 25 (2012) 434.

[43] Y. Jiao, A. Du, S. C. Smith, Z. Zhu, S. Z. Qiao, H_2 purification by functionalized graphdiyne-role of nitrogen doping, J. Mater. Chem. A 3 (2015) 6767-6771.

[44] Y. B. Apriliyanto, M. N. F. Lago, A. Lombardi, S. Evangelisti, M. Bartolomei, T. Leininger, F. Pirani, Nanostructure selectivity for molecular adsorption and separation: the case of graphyne layers, J. Phys. Chem. C 122 (2018) 16195-16208.

[45] C. Zhu, H. Li, X. C. Zeng, E. G. Wang, S. Meng, Quantized water transport: ideal desalination through graphyne-4 membrane, Sci. Rep. 3 (2013) 3163.

[46] J. Kou, X. Zhou, H. Lu, F. Wu, J. Fan, Graphyne as the membrane for water desalination, Nanoscale 6 (2014) 1865-1870.

[47] M. Raju, Pavan B. Govindaraju, Adri C. T. van Duin, M. Ihme, Atomistic and continuum scale modeling of functionalized graphyne membranes for water desalination, Nanoscale 10 (2018) 3969-3980.

[48] X. Gao, J. Zhou, R. Du, Z. Xie, S. Deng, R. Liu, Z. Liu, J. Zhang, Robust superhydrophobic foam: a graphdiyne-based hierarchical architecture for oil/water separation, Adv. Mater. 28 (2016) 168.

[49] R. Liu, J. Zhou, X. Gao, J. Li, Z. Xie, Z. Li, S. Zhang, L. Tong, J. Zhang, Z. Liu, Graphdiyne filter for decontaminating lead-ion-polluted water, Adv. Electron. Mater. 3 (2017) 1700122.

[50] G. Li, Y. Li, H. Liu, Y. Guo, Y. Li, D. Zhu, Architecture of graphdiyne nanoscale films, Chem. Commun. 46 (2010) 3256-3258.

[51] J. Li, Z. Xie, Y. Xiong, Z. Li, Q. Huang, S. Zhang, J. Zhou, R. Liu X. Gao, C. Chen, L. Tong, J. Zhang, Z. Liu, Architecture of β-graphdiyne-containing thin film using modified glaser-hay coupling reaction for enhanced photocatalytic property of TiO_2, Adv. Mater. 29 (2017) 1700421.

[52] Q. Li, Y. Li, Y. Chen, L. Wu, C. Yang, X. Cui, Synthesis of γ-graphyne by mechanochemistry and its electronic structure, Carbon 136 (2018) 248-254.

[53] G. Kresse, J. Furthmüller, Efficient iterative schemes for *ab initio* total-energy calculations using a plane-wave basis set, Phys. Rev. B 54 (1996) 11169.

[54] J. P. Perdew, K. Burke, M. Ernzerhof, Generalized gradient approximation made simple, Phys. Rev. Lett. 77 (1996) 3865.

[55] A. Togo, I. Tanaka, First principles phonon calculations in materials science, Scr. Mater. 108 (2015) 1-5.

[56] X. Kong, L. Li, O. Leenaerts, X. Liu, F. M. Peeters, New group-V elemental bilayers: A tunable structure model with four-, six-, and eight-atom rings, Phys. Rev. B 96 (2017) 035123.

[57] J. Wang, S. Deng, Z. Liu, Z. Liu, The rare two-dimensional materials with Dirac cones, Natl. Sci. Rev. 2 (2015) 22-39.

[58] H. Bu, M. Zhao, H. Zhang, X. Wang, Y. Xi, Z. Wang, Isoelectronic doping of graphdiyne with boron and nitrogen: stable configurations and band gap modification, J. Phys. Chem. A 116 (2012) 3934-3939.

[59] Z. Wang, X. Zhou, X. Zhang, Q. Zhu, H. Dong, M. Zhao, A. R. Oganov, Phagraphene: a low-energy graphene allotrope composed of 5-6-7 carbon rings with distorted Dirac cones, Nano Lett. 15 (2015) 6182-6186.

[60] X. He, J. Tan, H. Bu, H. Zhang, M. W. Zhao, The roles of π electrons in the electronic structures and optical properties of graphyne, Chin. Sci. Bull. 57 (2012) 3080-3085.

[61] J. Heyd, G. E. Scuseria, M. Ernzerhof, Hybrid functionals based on a screened Coulomb potential, J. Chem. Phys. 118 (2003) 8207.

[62] J. Heyd, G. E. Scuseria, M. Ernzerhof, Erratum: "Hybrid functionals based on a screened Coulomb potential" [J. Chem. Phys. 118, 8207 (2003)], J. Chem. Phys. 124 (2006) 219906.

Figure captions

Fig.1: (a) Structure of $T_{4,4,4}$-graphyne monolayer in top and side view. The brown spheres and sticks represent atoms and bonds, respectively, d_1-d_6 denote six different bond lengths, l labels the diameter of circumcircle of 18-carbon ring, and the blue dashed quadrangle indicates the unite cell. (b) Phonon dispersion curves of $T_{4,4,4}$-graphyne monolayer with $3 \times 3 \times 1$ supercell.

Fig.2: Thermal stability of $T_{4,4,4}$-graphyne. (a)-(c) Total energy fluctuations of $T_{4,4,4}$-graphyne monolayer at 500 K, 1000 K, and 1500 K, respectively. (d)-(e) The corresponding snapshots (top view) for equilibrium structures of $T_{4,4,4}$-graphyne monolayer at the end of 5 ps MD simulations.

Fig.3: Orbital-projected band structure of monolayer $T_{4,4,4}$-graphyne from PBE calculation (solid curves) in which the blue and pink solid curves represent the contributions from p_z and $s + p_x + p_y$ atomic orbitals of carbon atoms, respectively. The band structure of monolayer $T_{4,4,4}$-graphyne from TB model is depicted by green dashed curves.

Fig.4: Band structures of monolayer $T_{4,4,4}$-graphyne from HSE06 calculation.

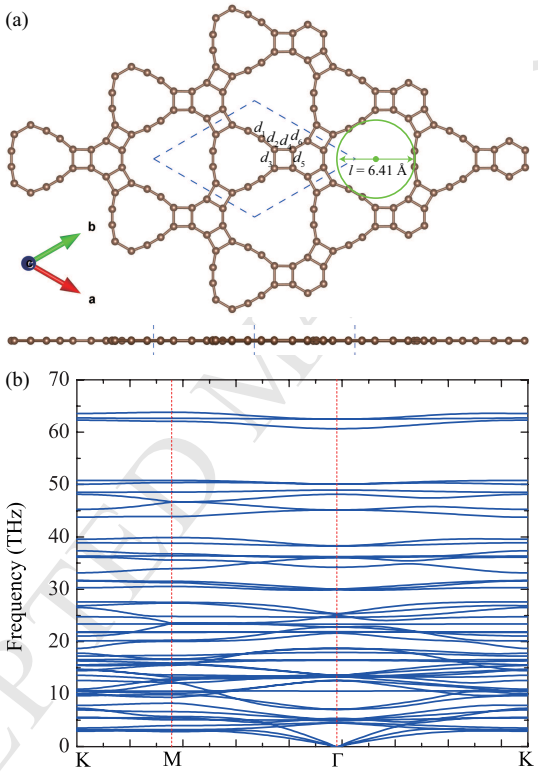

Figure 1: (Color online) (a) Structure of $T_{4,4,4}$-graphyne monolayer in top and side view. The brown spheres and sticks represent atoms and bonds, respectively, d_1-d_6 denote six different bond lengths, l labels the diameter of circumcircle of 18-carbon ring, and the blue dashed quadrangle indicates the unite cell. (b) Phonon dispersion curves of $T_{4,4,4}$-graphyne monolayer with $3 \times 3 \times 1$ supercell.

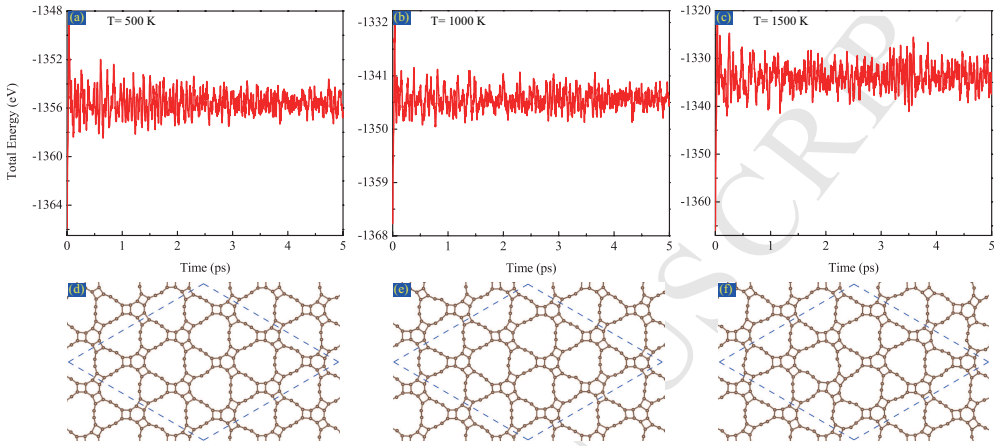

Figure 2: (Color online) Thermal stability of $T_{4,4,4}$-graphyne. (a)-(c) Total energy fluctuations of $T_{4,4,4}$-graphyne monolayer at 500 K, 1000 K, and 1500 K, respectively. (d)-(e) The corresponding snapshots (top view) for equilibrium structures of $T_{4,4,4}$-graphyne monolayer at the end of 5 ps MD simulations.

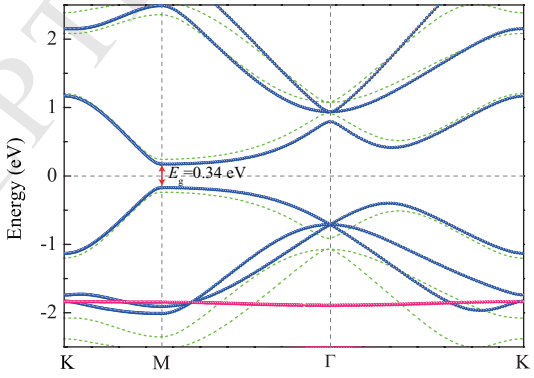

Figure 3: (Color online) Orbital-projected band structure of monolayer $T_{4,4,4}$-graphyne from PBE calculation (solid curves) in which the blue and pink solid curves represent the contributions from p_z and $s + p_x + p_y$ atomic orbitals of carbon atoms, respectively. The band structure of monolayer $T_{4,4,4}$-graphyne from TB model is depicted by green dashed curves.

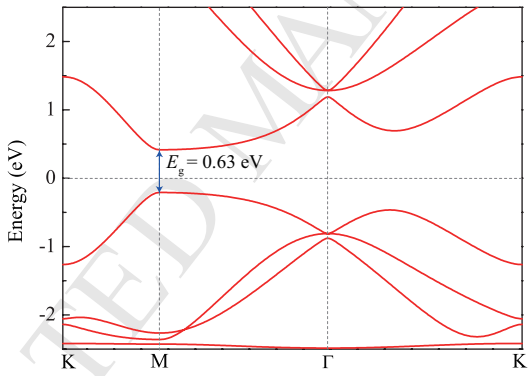

Figure 4: (Color online) Band structures of monolayer $T_{4,4,4}$-graphyne from HSE06 calculation.

Highlights

> Forming a nanoporous structure with a pore size of 6.41 Å. > Exhibiting a direct bandgap of 0.63 eV. > A promising material for water purification and for electronic devices. > Energetically more preferable than the experimentally realized β-graphdiyne.